Pharmaceutical Research (2022) 39:3197–3208
https://doi.org/10.1007/s11095-022-03416-6

ORIGINAL RESEARCH ARTICLE

Densifying Co-Precipitated Amorphous Dispersions to Achieve Improved Bulk Powder Properties

Derek S. Frank[1] · Ashish Punia[2] · Mairead Fahy[3] · Chad Dalton[4] · Jasmine Rowe[4] · Luke Schenck[1]

Received: 25 July 2022 / Accepted: 11 October 2022 / Published online: 21 October 2022
© Merck & Co., Inc., Rahway, NJ, USA and its affiliates 2022

Abstract

Purpose Precipitation of amorphous solid dispersions has gained traction in the pharmaceutical industry given its application to pharmaceuticals with varying physicochemical properties. Although preparing co-precipitated amorphous dispersions (cPAD) in high-shear rotor–stator devices allows for controlled shear conditions during precipitation, such aggressive mixing environments can result in materials with low bulk density and poor flowability. This work investigated annealing cPAD after precipitation by washing with heated anti-solvent to improve bulk powder properties required for downstream drug product processing.

Methods Co-precipitation dispersions were prepared by precipitation into pH-modified aqueous anti-solvent. Amorphous dispersions were washed with heated anti-solvent and assessed for bulk density, flowability, and dissolution behavior relative to both cPAD produced without a heated wash and spray dried intermediate.

Results Washing cPAD with a heated anti-solvent resulted in an improvement in flowability and increased bulk density. The mechanism of densification was ascribed to annealing over the wetted T_g of the material, which lead to collapse of the porous co-precipitate structure into densified granules without causing crystallization. In contrast, an alternative approach to increase bulk density by precipitating the ASD using low shear conditions showed evidence of crystallinity. The dissolution rate of the densified cPAD granules was lower than that of the low-bulk density dispersions, although both samples reached concentrations equivalent to that of the spray dried intermediate after 90 min dissolution.

Conclusions Hot wash densification was a tenable route to produce co-precipitated amorphous dispersions with improved properties for downstream processing compared to non-densified powders.

Keywords amorphous dispersion · annealing · co-precipitation · co-processed API · microprecipitated bulk powder

Introduction

Amorphous solid dispersions (ASDs) are a well-established formulation approach to improve the dissolution rate and oral bioavailability of poorly water-soluble pharmaceuticals. [1–4] However, material attributes of ASDs are sensitive to processing conditions and can plague downstream oral solid dosage form manufacture.[5–7] For instance, although spray drying is a common manufacturing method to produce ASDs in an commercial setting,[8] the resulting powder often possesses variable particle morphology and non-ideal bulk properties,[9–13] resulting in poor powder flow that challenges the manufacturing process. Additionally, small changes to spray drying process parameters can have an impact on the mechanical properties of the formulation. [14] Continuous unit operations to generate amorphous dispersions, such as hot melt extrusion and co-precipitation, offer improved control and reproducibility of bulk powder properties of amorphous dispersions[15–18] and can alleviate complexities involved with processing and technology transfer of spray drying manufacturing trains.[19–21] Due to the temperature requirements to achieve a homogeneous solid solution during melt extrusion, co-precipitation is

✉ Derek S. Frank
derek.frank@merck.com

1 Process Research & Development, Merck & Co., Inc., Rahway, NJ, USA

2 Analytical Research & Development, Merck & Co., Inc., Rahway, NJ, USA

3 Pharmaceutical Commercialization Technology, Merck & Co., Inc., Rahway, NJ, USA

4 Formulation Sciences, Merck & Co., Inc., Rahway, NJ, USA

preferred to generate amorphous dispersions for thermally labile pharmaceuticals.[22–24].

One challenge of co-precipitated amorphous dispersions (cPAD) can be low bulk density and poor flow properties. Additionally, while in some instances *in vitro* dissolution of cPAD particles and spray dried intermediate (SDI) are comparable, the wettability of cPAD bulk powder is often worse than SDI, which can challenge the ability to achieve a uniform suspension for formulations in toxicity studies or achieve complete dissolution.[25, 26] Previous work has investigated precipitation conditions[18] and downstream unit operations such as dry granulation[27, 28] to improve flow properties of cPAD. Recent work from our group demonstrated an approach to densify cPAD by briefly heating dispersions above their solvent-wetted glass transition temperatures.[29] This process was performed at scale using an in-line rotor stator mill coupled to a thin-film evaporator.[30] Processing by thin film evaporation resulted in improved bulk density and flow properties, allowing for direct compression of tablets at a reduced image size compared to a comparable formulation containing spray dried intermediate. Despite the promise of thin film evaporation and continuous manufacturing methods at commercial scale[17, 31], implementing this technology requires upfront capital costs and process optimization for successful operation. Particularly for the production of pharmaceutical supplies to support pre-clinical and early clinical studies, maximizing speed and minimizing cost are essential to inform probability-of-success for a new chemical entity. Given the importance of these constraints in early development, and the ability to generate cPAD using standard drug substance facilities,[32] we sought to investigate processes using commonly available laboratory equipment to densify co-precipitated amorphous dispersions and improve their bulk powder properties for small-scale deliveries.

Co-precipitated amorphous dispersions were prepared under a variety of conditions to identify sensitivities in the precipitation process to material attributes and powder properties. Pharmaceuticals celecoxib and Compound X, a Merck & Co., Inc., Rahway, NJ, USA compound, were studied as model compounds using hydroxypropyl methylcellulose acetate succinate (HPMCAS) and a poly(dimethylaminoethyl methacrylate) copolymer (Eudragit EPO) as polymeric stabilizers in the amorphous phase. Densification of cPAD was achieved by washing with heated anti-solvent, resulting in improved flow properties and dispersibility in aqueous suspensions (Fig. 1). Compared to other densification approaches, this hot wash method reduced risk to recrystallization of the cPAD and did not require the use of additional excipients for improved mechanical strength during tableting. Such work highlights the promise of novel solvent-based unit operations to optimize the powder properties of ASDs.

Materials/Methods

Materials

Compound X was synthesized by Merck & Co., Inc., Rahway, NJ, USA, celecoxib (> 98%, Sigma-Aldrich, St. Louis, MO, USA), HPMCAS-L (ShinEtsu, Japan), HPMCAS-M (ShinEtsu), Eudragit® EPO (Evonik, Darmstadt, Germany), acetone (Fisher Chemical, USA), ammonium hydroxide (10 vol%, Fisher Chemical), 5 N hydrochloric acid (Ricca, Arlington, TX, USA), *n*-heptane (Fisher Chemical), dimethylformamide (Fisher Chemical), dimethyl sulfoxide (Fisher Chemical), and dimethylacetamide (Fisher Chemical) were purchased from listed suppliers. Hydrochloric acid and ammonium hydroxide were diluted in deionized water prior to use.

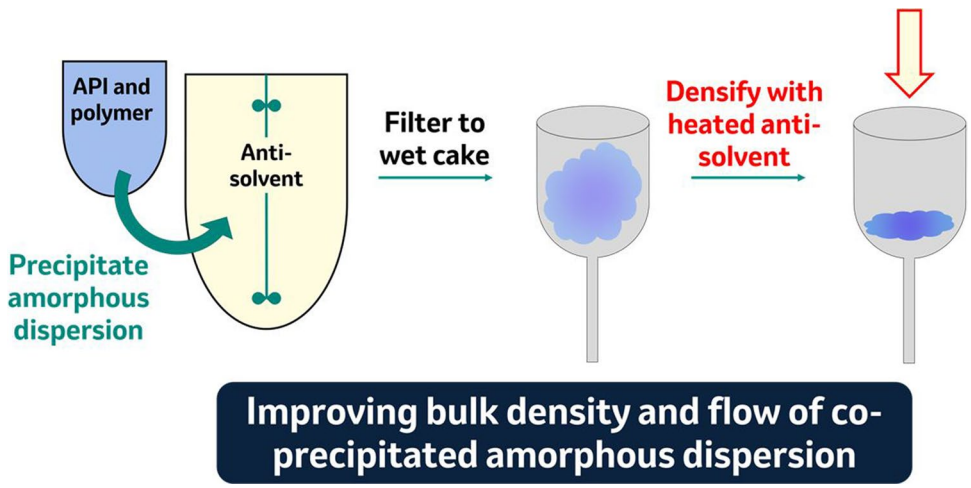

Fig. 1 Illustration depicting densification process for co-precipitated amorphous dispersions.

Solubility of Compound X

Solubility of Compound X in various anti-solvents and binary solvent/anti-solvent mixtures was assessed by agitating crystalline Compound X powder in solvents on a laboratory shaker (Glas-Col, Terre Haute, IN, USA) at ambient temperature (~ 20 °C). The slurry was then filtered through a 0.22 µm filter (Cytiva Life Sciences, Marlborough, MA USA) and diluted in acetonitrile before analysis by reverse-phase ultra-high performance liquid chromatography (1290 Infinity II LC System, Agilent, Santa Clara, CA, USA) using a C18 column (Ascentis Express C18 column, Sigma-Aldrich) and a 95:5 acetonitrile:0.1 vol% aqueous phosphoric acid mobile phase with UV detection at 210 nm. Equilibrium solubility at room temperature was measured for four separate samples with averages reported in the manuscript text.

Spray dried dispersions of Compound X

Spray dried intermediate was manufactured on a PSD-1 spray dryer (GEA Niro, Columbia, MD, USA) by dissolving API and HPMCAS in acetone (10 wt% solids loading) and spray drying at 15 L/hr at an inlet temperature of 119 °C. The obtained SDI was dried at 40 °C/15% RH for at least 12 h to remove residual solvent.

Preparing co-precipitated amorphous dispersions containing Compound X by precipitation into beaker

Compound X (40 g/L) and HPMCAS-L (93.3 g/L) were co-dissolved in acetone at elevated temperature (~ 40 °C, 10 ml solution overall). The solution was cooled to room temperature and manually added at ~ 5 mL/min into cooled anti-solvent (0.001 N HCl cooled to 5°C), either unagitated or stirred at 500 RPM by a magnetic stir bar, at a 1:10 solvent:anti-solvent ratio. The precipitated dispersion was filtered on a fritted funnel (10–15 µm pore size) with a nitrogen sweep and dried in a vacuum oven overnight at room temperature to remove residual solvent.

Preparing co-precipitated amorphous dispersions by overhead mixing

Compound X (40 g/L) and HPMCAS-L (93.3 g/L) were co-dissolved in solvent at elevated temperature (~ 40°C). The solution was cooled to room temperature and manually added at ~ 25 mL/min into the shear zone of a 0.001 N HCl anti-solvent agitated at 375 RPM by a OHS 20 Digital Overhead Stirrer (VELP Scientifica, Deer Park, NY, USA) at a 1:10 solvent:anti-solvent ratio. For precipitation from acetone, anti-solvent at either 5°C or 75°C was used to understand the impact of anti-solvent temperature on cPAD properties. For precipitation from dimethylacetamide (DMAc), anti-solvent was cooled to 5°C, and for precipitation for precipitation from dimethyl sulfoxide (DMSO), anti-solvent was controlled to 22°C to avoid freezing of solvent. The precipitated dispersions were filtered on a fritted funnel (10–15 µm pore size), displacement washed with an additional equivalent amount of anti-solvent (for DMAc and DMSO co-precipitations), and dried with a nitrogen sweep overnight at ambient temperature.

Preparing co-precipitated amorphous dispersions in Quadro HV0

API (40 g/L) and stabilizing polymer (93.3 g/L) were co-dissolved in acetone at elevated temperature (~ 40°C). The solution was cooled to room temperature and fed at ~ 150 mL/min into a Quadro HV0 homogenizer (Quadro Engineering Corp., Waterloo, ON, Canada) running at a tip speed of 30 m/s containing cooled 0.001 N HCl as anti-solvent for dispersions stabilized by HPMCAS and cooled 0.1 vol% ammonium hydroxide for ASDs containing Eudragit EPO at a 1:10 ratio of solvent:anti-solvent. The co-precipitated amorphous dispersion was isolated by filtration.

Hot wash densification

The co-precipitated amorphous dispersion was densified by washing the wet cake with anti-solvent heated to a specified temperature with a displacement wash. Approximately 1 L of anti-solvent was used per 15 g cPAD, although as discussed below, less anti-solvent may be required to densify the cPAD given sufficient annealing can be achieved at a given temperature. After densification, the cPAD was allowed to dry under a nitrogen sweep. Once dried, the powder was de-lumped through a 1 mm mesh screen to break apart aggregates.

Densification in oven

To understand the kinetics of densification, a sample of unwashed co-precipitated amorphous dispersion containing Compound X was also densified by annealing the wet cake in an oven set to 50°C after precipitation. After storage to pre-determined time points, the extent of densification was assessed qualitatively.

Drug load assay by UV vis spectrometry

Drug loading in the precipitation dispersions was determined by dissolving a known mass of amorphous dispersions in acetonitrile and calculating drug load by UV vis absorbance using an Agilent UV vis spectrometer (Cary 60, Agilent, Santa Clara, CA, USA). For Compound X, 294 nm was used

to quantify drug concentration; for celecoxib, 274 nm was used. Drug load was measured for two samples separately and is presented with standard deviation.

Powder X-ray diffraction (PXRD)

PXRD was performed on a Bruker D2-PHASER (Bruker, Madison, WI, USA) using a Cu tube radiation ($\lambda = 1.54184$ Å) at 30 kV and 10 mA between 5 and 40° 2θ with a 0.002° step size and 0.150 s/step. Data was visualized using X'Pert HighScore Plus software package (Malvern Panalytical Inc., Westborough, MA, USA).

Differential scanning calorimetry (DSC)

Thermal analysis was performed on a Q2000 DSC (TA Instruments, New Castle, DE) using hermetically sealed Tzero pans and lids with pinholes. The glass transition of dry cPAD was measured by pre-cooling samples below 50°C and heating at 3°C/min with a modulation of 1°C per 60 s. The glass transition of the wet cake samples (HPMCAS dispersions wetted with 0.001 N HCl and Eudragit EPO dispersions wetted with 0.1 vol% ammonium hydroxide) was measured by pre-cooling samples to at least 5°C and heating at 2°C/min with a modulation amplitude of 1.5°C per 60 s using hermetically sealed Tzero pans and lids. The glass transition temperature was identified by a step change in reversing heat flow. Melting point endotherms were measured in standard heating mode with a ramp rate of 5°C/min using hermetically sealed Tzero pans and lids with pinholes.

Particle size distribution

Particle size analysis was performed in deionized water using a Mastersizer 3000 (Malvern, Panalytical, United Kingdom) and analyzed using Mie scattering theory for non-spherical particles using 1.53 as an estimated refractive index, 0.1 as the absorption index of the amorphous dispersions, and 1.33 as refractive index for aqueous buffer. The aqueous dispersant to measure particle size of EPO dispersions was basified using a few drops of concentrated NaOH. Five measurements were collected per sample.

Flodex measurement

Powder flowability was assessed using the Flodex instrument (Hanson Research, CA). Approximately 70 mL of each powder was equilibrated at 30% RH in an open weigh boat. Flodex measurement was performed by charging the powder into the Flodex and recording the critical arching diameter where 50% of replicates flow and 50% of replicates arch, which is reported in the text with ± 2 mm error.

Scanning electron microscopy

Scanning electron micrographs were collected using a Hitachi TM3030 Tabletop Microscope (Hitachi High-Technologies Corporation, Tokyo, Japan) at 15 kV voltage.

Bulk Density

Bulk density of cPAD powders was measured using a 10 mL graduated cylinder. A known volume of powder was filled into the graduated cylinder, and the weight of the filled power was measured using a pre-tared analytical balance. The bulk density was calculated by dividing the mass of the powder by the volume.

Compressibility and strength of cPAD compacts

Tabletability profiles of neat cPAD were generated to evaluate suitability of hot washed cPAD for downstream tablet compression. A single-stage compaction simulator (Roland Research Devices Inc., Ewing, NJ) using 3/8″ round flat faced tooling was used to generate 10 compacts of approximately 300 mg compressing weight using compression pressures ranging from 50 to 500 MPa. Powder was hand filled into the die to ensure compact weight. Weight, thickness, diameter, and hardness of compacts was measured using a SOTAX ST50 (SOTAX Corp., Westborough, MA, USA). Tensile strength (*TS*) of compacts produced by each compressive force was calculated by the below equation with F_B is the peak force at breaking, t the tablet thickenss, and D the tablet diameter. Actual compression pressure applied was recorded by the compaction simulator software and used to generate a tabletability profile.

$$TS = \frac{2F_B}{\pi t D}$$

Dispersibility and dissolution rate of Compound X ASDs

Dispersibility was assessed by charging 75 mg of cPAD into 7.5 mL 0.001 N HCl and shaking by hand. Images of the dispersed material are shown in the manuscript text after 30 s to allow for powder settling.

Dissolution of amorphous solid dispersions was performed in a two-stage dissolution procedure by initially charging 100 µg/mL API-equivalent dose into pH 1.6 simulated gastric buffer, dispersing for 30 min, followed by dilution to 50 µg/mL concentration with the addition of an equal volume of neutral buffer solution containing 6.88 g/L NaH_2PO_4 of sodium phosphate monobasic

(anhydrous), 10.37 g/L NaCl, and dilute NaOH such that a 1:1 mixture of SGF and the buffer solution had a pH of 6.5. This concentration was selected as it is below the amorphous solubility of Compound X in FaSSIF (90 µg/mL), allowing for differentiation between the samples.

Specific surface area measurement

Specific surface area was measured using the Brunauer, Emmett, Teller (BET) isotherm method using a Micromeritics TriStar II 3020 (Micromeritics, Norcross, GA, USA) surface area analyzer. For BET analysis, the amount of nitrogen gas that was adsorbed in the relative pressure (P/Po) range from 0.08 to 0.3 was used (containing a total of 9 relative pressure points) with an equilibration time of 5 s. Approximately 0.5 g sample quantity was used for each measurement and prior to the analysis sample degassing was performed under nitrogen flow for approximately 2 h at 35°C.

Table I Solubility of Compound X in Various Anti-Solvent and Anti-Solvent/Solvent Binary Pairs to Assess Feasible Conditions for Co-Precipitation and Densification (Average of Four Separate Measurements with Standard Deviation)

Solvent	Solubility of crystalline Compound X at room temperature (µg/mL)
0.001 N HCl	< 1
10 vol% acetone in 0.001 N HCl	1.2 ± 0.1
n-heptane	< 1
10 vol% acetone in *n*-heptane	4.3 ± 0.4
Methyl tert butyl ether	208 ± 0.1
Acetone[a]	48,000

[a]Extrapolated from Van't hoff equation by measuring solubility at various temperatures (see Figure S1)

Results/Discussion

The solubility of Compound X was measured in anti-solvents and binary mixtures of solvent and anti-solvent to inform processing conditions to produce and densify co-precipitated materials. Shown in Table I, crystalline Compound X had low solubility in anti-solvents 0.001 N HCl and *n*-heptane. Adding 10 vol% acetone to the acidified water anti-solvent increased the API solubility to roughly 1 µg/mL, whereas addition of 10 vol% of acetone to *n*-heptane had a more pronounced effect and increased solubility to > 4 µg/mL. Such observations are in line with historical process development of Compound X cPAD (see Table S1 in Supporting Information), where precipitation into *n*-heptane resulted in the extraction of API from the amorphous dispersion.

Impact of mixing conditions during precipitation on crystalline content

The shear environment used to mix solvent and anti-solvent was correlated with distinct material attributes of the resulting co-precipitated dispersion. Although rapid mixing can be necessary to produce kinetic phases by precipitation,[33] aggressive shear during co-precipitation can result in low bulk density particles. Co-precipitation was performed under four conditions: dropwise addition of solvent into anti-solvent in an unagitated beaker, dropwise addition into a beaker with agitation from a magnetic stir bar, dropwise addition with agitation by an over-head stirrer, and feeding into the shear-zone of an in-line wet mill homogenizer, representing shear rates ranging over at least 3-orders of magnitude.[34] Characterization of these cPAD materials and a spray dried intermediate of the same composition is shown in Table II. The unstirred precipitation yielded a material with residual crystallinity, in contrast to precipitations in the presence of a shear field. Crystallinity in the dispersion was measurable by PXRD as well as indicated by a melt endotherm at high temperature by DSC. The material also had a bulk density of approximately 0.3 g/cc, greater than that of the SDI or

Table II Material Attributes of Target 30% DL Compound X in HPMCAS-L ASDs Prepared by Co-Precipitation and Spray Drying

Processing Conditions	%Drug Load	T_g (°C)	PXRD	Bulk Density (g/cc)	ΔH_{melt} (J/g)/T_m (°C)
Co-precipitation without agitation (5°C)	29.1 ± 1.2	102.6	Partial crystallinity	0.3	4.92/235
Co-precipitation with magnetic stir bar (5°C)	30.0 ± 1.0	99.0	Amorphous	< 0.1	2.04/238
Co-precipitation with overhead agitator (5°C)	29.4 ± 0.7	99.5	Amorphous	< 0.1	0.71/239
Co-precipitation with in-line rotor–stator (5°C)	30.1 ± 0.5	99.6	Amorphous	< 0.1	not observed
Co-precpitation with overhead agitator (75°C)	27.2 ± 0.1	100.5	Amorphous	0.13	1.68/235
Spray drying	30.2	98.3	Amorphous	0.23	not observed

cPAD formed under agitation. One possible mechanism for both higher bulk densities as well as crystallization for the unstirred cPAD was solvent-induced plasticization during precipitation.[29] Without adequate convective mixing, the co-precipitated dispersion contained entrained solvent after precipitation which was later removed by drying by a nitrogen sweep. In contrast, co-precipitation in the presence of a shear field produced amorphous material. Mixing with a magnetic stir bar during the precipitation produced a material without crystallinity by PXRD; however, this material showed a melt endotherm at elevated temperature, possibly signifying low levels of residual crystallinity in the dispersion or amorphous nanostructure primed to undergo crystallization while heating during DSC analysis. cPAD prepared at higher shear rates using an overhead agitator showed reduced crystallinity by DSC, and no crystallinity was observed for material prepared using an in-line rotor–stator wet mill. This difference between the precipitates indicates that the shear conditions during co-precipitation can impact residual crystallinity in the dispersion. However, one downside to higher shear rates was that the bulk density of the cPAD was below 0.1 g/cc. The high shear rates and turbulent mixing appeared to reduce bulk density of the precipitate, a phenomenon which has been observed for other cPAD materials generated in a similar fashion.[35] Co-precipitation was also performed at 75°C to understand sensitivities to temperature. At a higher temperature, cPAD had 27.2% drug load (91% label claim) and a glass transition temperature (T_g) of 100.5°C. The loss of drug from the cPAD during co-precipitation was likely due to elevated solubility of Compound X in mother liquors at high temperature. There was no evidence of crystallinity in the amorphous dispersion, although DSC analysis showed a melt endotherm at elevated temperature. Additionally, this dispersion had improved bulk density relative to those prepared at lower temperatures. Similar amorphous materials were prepared using dimethyl sulfoxide (DMSO) or dimethylacetamide (DMAc) as solvents, indicating a limited impact of solvent on the solid-state properties of the co-precipitated dispersion (see Table S2 in Supporting Information). Qualitative properties of the cPAD material such as bulk density were also unchanged by using DMAc or DMSO as opposed to acetone.

Impact of a heated anti-solvent wash on bulk powder properties

Although a high shear rate was effective to generate fully amorphous co-precipitate, the material attributes of this cPAD were not ideal for formulation. The bulk density of the Compound X co-precipitate was less than 0.1 g/cc and flowability was poor. Following previous work investigating densification of co-precipitated materials, cPAD was densified by washing with heated anti-solvent to briefly plasticize the cPAD above its wetted glass transition temperature.[29] This hot wash method allowed for rapid heating and cooling of the cPAD in the presence of residual aqueous anti-solvent, which was preferred over slower heat transfer methods such as secondary drying. Additionally, washing with heated anti-solvent did not result in crystallization or any drug extraction from the cPAD. Both heated *n*-heptane and heated acidified water were able to densify the cPAD wet cake, although it was necessary to remove residual solvent to prevent extraction of API during the wash process (see Table S3 in Supporting Information).

Table III details material attributes before and after densification including particle size, bulk density, Flodex coefficient, and specific surface area. The flow properties of the unprocessed cPAD were poor and a Flodex minimum diameter could not be measured. Densification via a hot wash improved bulk density and flow properties. Shown in Table III, densification at 60°C provided an increase in bulk density to > 0.1 g/cc. Although flow properties of the cPAD were also improved upon densification at this temperature, the Flodex coefficient for material washed at 60°C was similar to spray dried intermediate (23 mm *vs* 21 mm). However, washing cPAD with anti-solvent heated to 75°C provided a further improvement in flow properties of the material (Flodex minimum diameter of 11 ± 2 mm). Figure 2 compares microstructure of cPAD by scanning electron microscopy

Table III Material Attributes of 30% DL Compound X in HPMCAS-L ASDs prepared by Co-Precipitation, Spray Drying, and Co-Precipitation with a Hot Wash. D_{10}, D_{50}, and D_{90} Particle Sizes are Given as an Average of Five Measurements with Standard Deviation

Processing Conditions	D_{10} (μm)	D_{50} (μm)	D_{90} (μm)	Bulk Density (g/cc)	Flodex	Specific Surface Area (m^2/g)
Spray dried dispersion	9.9 ± 0.3	27.8 ± 0.1	61.0 ± 0.9	0.23	21 ± 2 mm	not measured
Co-precipitation with in-line rotor–stator	15.5 ± 0.2	67.7 ± 1.4	202 ± 4	< 0.1	> 34 mm	15.73 ± 0.12
Co-precipitation with in-line rotor–stator and 60°C anti-solvent wash	38.7 ± 0.4	181 ± 2	696 ± 19	0.13	23 ± 2 mm	not measured
Co-precipitation with in-line rotor–stator and 75°C anti-solvent wash	64.3 ± 0.9	221 ± 2	413 ± 7	0.14	11 ± 2 mm	2.27 ± 0.05

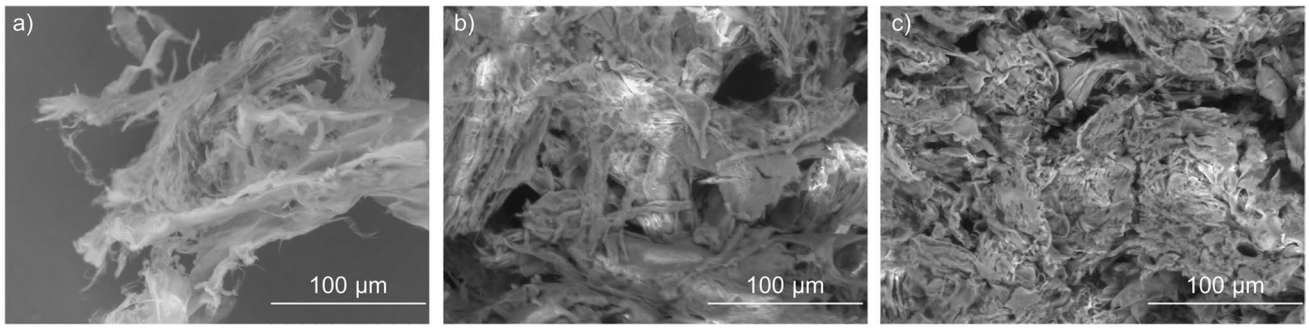

Fig. 2 Scanning electron micrographs of co-precipitated dispersions containing Compound X (**a**) without densification, (**b**) washed with 60°C anti-solvent, and (**c**) washed with 75°C anti-solvent.

after washing at various temperatures to understand these differences in powder attributes. Before densification, the cPAD material was composed of porous fibers with a specific surface area of 15.73 ± 0.12 m^2/g (Table II). Densification with a hot wash mediated collapse of these fibers; cPAD densified at 60°C (Fig. 2b) showed fusion of these fibers into larger particles, although it also contained flat sheets of ASD which may have contributed to cohesive interactions in the material. Densification at 75°C (Fig. 2c) further collapsed cPAD into aggregates, resulting in a decrease in specific surface area of the material to 2.27 ± 0.05 m^2/g. This corresponded with an increase in the median particle size from 67 µm to 181 µm, reflecting agglomeration of cPAD primary particles, while SEM also showed altered surface features suggesting annealing. Both particle size and shape impact the flow properties of a powder[36–38], and it is possible that the increase in particle size as well as the altered morphology of the cPAD upon densification mediated improvements in flowability. Furthermore, despite these improvements in bulk powder properties achieved upon densification, no evidence of crystallization was observed in the densified cPAD by DSC analysis (see Figure S2 in Supporting Information).

Wettability and dissolution of the cPAD powder was compared before and after densification. As illustrated in Fig. 3, densified cPAD showed improved dispersibility into aqueous media. The non-densified cPAD floated on the surface of the aqueous suspension (Fig. 3). In contrast, the densified material readily redispersed in the suspension, similar to the spray dried amorphous dispersion. Similar improvements in dispersibility have been achieved with a hierarchical particle approach, where water-soluble excipients are coated onto cPAD during drying.[25, 35] This improvement in dispersibility might allow for dosing aqueous suspensions in toxicity studies by gavage. Additionally, dissolution of the cPAD powder was performed into simulated gastric buffer followed by dilution to pH 6.5 phosphate buffer (Fig. 4). The spray dried intermediate showed the fastest drug release in the first five minutes of dissolution at neutral pH. After 15 min

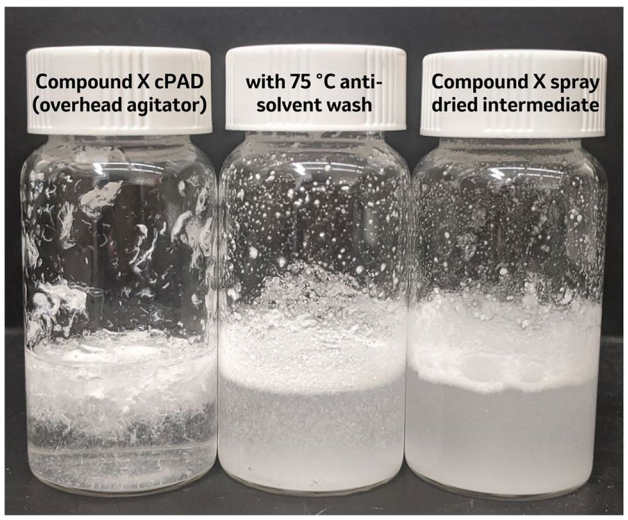

Fig. 3 Dispersibility of Compound X ASD generated by (from left to right) precipitation using an overhead agitator, precipitation from an in-line rotor–stator followed by a 75°C anti-solvent wash, and spray drying in deionized water.

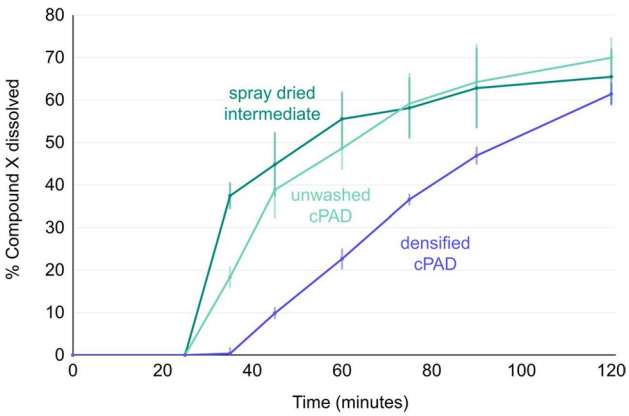

Fig. 4 Dissolution comparison between Compound X (30% DL in HPMCAS-L) spray dried intermediate (dark teal), unwashed co-precipitated dispersions (light teal), and densified cPAD (blue). The first 30 min of dissolution were in SGF, followed by dilution to neutral pH. Average of three dissolution trials is plotted with standard error.

of dissolution at neutral pH, the unwashed co-precipitated dispersion reached equivalent concentrations to the SDI. The densified cPAD showed slower release in neutral conditions, possibly due to the large particle size of the dispersed powder. Nevertheless, at 120 min of dissolution, all three materials showed approximately 60% drug release. Although a full pharmacokinetic study would be necessary to understand if these differences in dissolution rate impact *in vivo* exposure, previous pharmacokinetic studies comparing spray dried intermediate and cPAD densified by thin film evaporation showed equivalent performance for both materials.[30].

Informed by process development for Compound X, amorphous dispersions containing celecoxib were generated by co-precipitation to understand if hot wash densification can be a compound agnostic approach to improve bulk density and flow properties of cPAD. HPMCAS-M and Eudragit EPO were employed as stabilizers in the dispersions to investigate the impact of polymer T_g on densification and flow properties. Co-precipitated dispersions of celecoxib in HPMCAS-M (30% DL) were generated by precipitation from acetone into 0.001 N HCl. Shown in Table IV, similar to dispersions containing Compound X, the celecoxib cPAD powder had low bulk density and poor flow properties. Washing with 60°C acidified water did not result in a large improvement to bulk density or flowability. Washing with 75°C anti-solvent improved bulk density to greater than 0.1 g/cc and decreased the Flodex arching flow diameter to 17 mm. Additionally, for celecoxib/HPMCAS cPAD samples, specific surface area was measured for the undensified material and the sample washed with 75°C anti-solvent. The specific surface area of the cPAD decreased from 13.7 ± 0.02 m^2/g to 2.2 ± 0.03 m^2/g upon densification at 75°C, similar to changes observed for Compound X cPAD, highlighting a decrease in surface area as one potential mechanism of improved powder attributes the densified cPAD. Co-precipitated amorphous dispersions containing celecoxib and the basic copolymer Eudragit EPO were generated by precipitation from acetone into alkaline aqueous media (0.1 vol% aqueous ammonium hydroxide) and had a T_g of 53°C. Although the Eudragit EPO cPAD also had poor bulk density and flow properties directly after precipitation, hot wash densification at 60°C resulted in an improvement in bulk density (to 0.26 g/cc) and flow properties (Flodex arching diameter of 9 mm) without extraction of API or crystallization of the cPAD. Furthermore, similar to Compound X cPAD, densification with a hot wash resulted in an increase in particle size (see Figure S20 for scanning electron micrographs illustrating aggregation of the cPAD after hot wash densification). These data illustrate that densification approaches by annealing cPAD with a hot wash can be applied across pharmaceuticals and polymeric stabilizers, and that there is a relationship between temperatures required for an improvement in bulk powder properties and the polymer stabilizer used in the ASD.

Compaction performance of the densified cPAD powders was assessed by measuring tabletability profiles of the neat materials (Fig. 5). Profiles were not generated for unwashed materials due to their low bulk density. All three ASDs

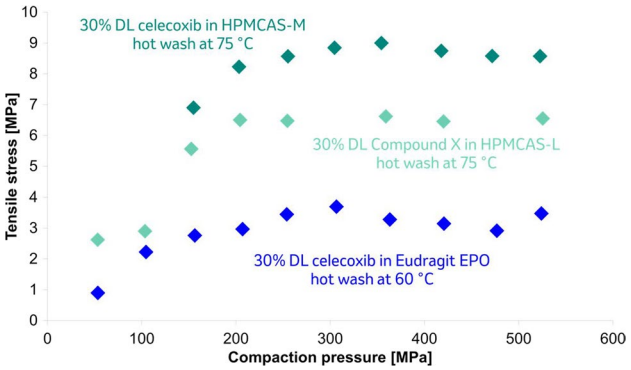

Fig. 5 Tensile strength as a function of compressive stress for washed 30% DL cPAD containing celecoxib in HPMCAS-M (dark teal), Compound X in HPMCAS-L (light teal), and celecoxib in Eudragit EPO (blue).

Table IV Material attributes of celecoxib cPAD including drug loading in dispersion, particle size distribution (with standard deviation), bulk density, and Flodex measurement

cPAD Material (API/Polymer)	Processing Conditions	%Drug Load	T_g (°C)	D_{10} (μm)	D_{50} (μm)	D_{90} (μm)	Bulk Density (g/cc)	Flodex
30% DL Celecoxib in HPMCAS-M	In-line rotor–stator	29.7 ± 0.6	84.7	15.4 ± 0.2	76.8 ± 1.3	252 ± 11	0.04	> 34 mm
	In-line rotor–stator with 60°C anti-solvent	29.9 ± 0.6	85.0	24.0 ± 0.5	118 ± 1.3	345 ± 10	0.06	33 ± 2 mm
	In-line rotor–stator with 75°C anti-solvent	29.0 ± 1.0	84.5	49.5 ± 1.6	220 ± 2	613 ± 16	0.12	17 ± 2 mm
30% DL Celecoxib in Eudragit EPO	In-line rotor–stator	29.9 ± 0.3	53.2	10.7 ± 0.2	38.9 ± 0.7	88.7 ± 1.7	0.03	32 ± 2 mm
	In-line rotor–stator with 60°C anti-solvent	29.6 ± 2.0	53.3	17.5 ± 0.3	85.9 ± 2.3	644 ± 25	0.26	7 ± 2 mm

showed sufficient tensile strength to indicate robust tableting behavior without the addition of mechanical strength enhancers or other compaction aid excipients. This compaction behavior, in tandem with favorable flow properties, may allow for direction compression of tablets containing the densified cPAD material, similar to tablets generated using cPAD densified by thin film evaporation.[30] Such results suggest that hot wash densification may be an effective approach to enable direction compression and minimize tablet burden for amorphous dosage units.

Comparison to other densification approaches and mechanism of powder densification during the hot-wash process

Previous work has offered alternative pathways to improve mechanical properties of co-precipitated amorphous dispersions. For instance, Hou, *et al.* generated co-precipitated dispersions by overhead mixing. These cPAD had reduced surface area relative to those generated by resonant acoustic mixing, which the authors linked to improved flow properties and bulk density.[18] A similar low surface area co-precipitate morphology was generated by Bhujbal, *et al*. [39] which showed bulk densities > 0.3 g/cc. Although improved bulk densities can be obtained by dropwise co-precipitation of Compound X, there was risk of crystallinity in the dispersion. This crystallization risk was hypothesized to originate from poor mixing between solvent and anti-solvent resulting in solvent entrainment in the ASD. Plasticization by residual solvent during secondary drying of ASDs has also been observed as a mechanism of crystallization during processing of spray dried dispersions.[40, 41] In contrast, higher shear processes to generate the amorphous phase resulted in a low bulk density material but improved mixing between solvent and anti-solvent and reduced evidence of crystallinity. Although low-shear co-precipitation may be appropriate for compounds with low crystallization propensity, a more rapid crystallizer such as Compound X can be sensitive to mixing conditions during precipitation. An additional advantage to precipitation in rotor–stator wet mills is that such devices can be integrated into manufacturing processes in a recycle loop to independently control the shear environment of a precipitation for varying batch sizes.[42, 43] It is unclear to what extent low-shear precipitation and drying conditions can be controlled at large-scale to ensure reproducible cPAD properties. Another method to densify cPAD is by dry powder slugging, which was investigated as an analog to roller compaction.[27] That said, this process required the use of Avicel as a dry binder to enhance mechanical strength in the formulation, which can result in increased tablet burden, in contrast to direct compression of densified ASDs.[30].

Annealing amorphous materials above their glass transition can cause risks to physical stability.[44] Previous work densifying co-precipitated dispersions by heating in a thin film evaporator resulted in favorable densification but also a reduction in physical stability of the densified cPAD under stressed storage conditions. In such work, cPAD was annealed in the thin film evaporator with a residence time of 10 min at approximately 80°C under vacuum to remove mother liquors and densify the co-precipitate. Though the thin film evaporated material demonstrated favorable flow properties and particle size allowing for direct compression of dosage units, and did not show crystallinity by PXRD at t = 0, the elevated densification temperatures correlated with in reduced physical stability under accelerated storage conditions (40°C/75% RH). In contrast, this hot wash densification approach used lower temperatures and shorter thermal exposure to densify cPAD. Hot wash densified cPAD showed limited evidence of crystallization during DSC in comparison to the TFE-processed material (see Figure S2 and Figure S3, Supporting Information). These data imply that there may be a trade-off between aggressive densification conditions leading to favorable powder properties and physical stability. Controlling the temperature and duration of washing with hot anti-solvent may mitigate risks of phase transformation during processing.

Despite a 15°C difference in T_g between cPAD containing celecoxib (T_g ~ 85°C) *versus* Compound X (T_g ~ 100°C), both materials required a 75°C hot wash to achieve improved flow and bulk density relative to the unwashed cPAD. The T_g for 30% DL Compound X cPAD wet cake was measured to be ~ 40°C, in line with previous analysis [30], and the wet cake T_g for 30% DL celecoxib cPAD was ~ 36°C (see Figure S19a in Supporting Information). Although there was a 15°C difference in dry T_g for each material, similarities in the wetted T_g may account for the similar requirements for densification temperature to achieve improved flowability. Additionally, low wetted T_g values relative to required densification temperatures implied that the collapse and agglomeration of cPAD fibers does not occur instantaneously above the T_g. To assess the kinetics of densification, Compound X cPAD wet cake was heated in an oven set to 50°C. After 10 min of annealing at 50°C, little densification was observed, whereas 30 min of annealing provided sufficient time for densification of the powder. The requirement of an anti-solvent hot wash to be above the wetted T_g suggests that the kinetics of cPAD densification vary with temperature above T_g, and that densification may be a function of temperature-dependent parameters such as viscosity of an amorphous material.[45] In line with these observations, the wet T_g of the celecoxib/EPO cPAD was measured to be ~ 26°C (see Figure S19b), and efficient densification was observed using an anti-solvent wash at 60°C. These data suggest

that annealing at least 35°C over the wet T_g is sufficient to achieve densification of cPAD powders with a hot anti-solvent wash. Furthermore, although heating cPAD above its T_g did not result in extraction or crystallization for Compound X or celecoxib, such a procedure may not be tenable for pharmaceuticals with rapid crystallization propensity in the solid-state. That said, the crystallization rate of amorphous materials is sensitive to temperature.[44, 46] For ASDs containing drug heavily diluted in polymer (as is often necessary for long-term storage stability and rapid dissolution performance of ASDs [47]), there may be lower risk to briefly heating cPAD during densification as compared to long term stressed storage testing used de-risk physical stability for manufacturing and commercialization.[48] Based on the above data, hot-wash densification of cPAD at least 35°C above the wetted T_g can mediate an improvement in bulk powder properties, and without a direct measurement of the wet T_g for an ASD, 75°C may be an appropriate densification temperature for dispersions stabilized by HPMCAS[49]. If such processing temperatures induce recrystallization in the cPAD, annealing for a longer duration at lower temperatures may yield a similar improvement to bulk powder properties.

Conclusion

Challenges associated with developing enabled formulations of poorly-soluble drug candidates can lead to lengthy manufacturing timelines and increased costs relative to conventional formulation approaches.[50] Co-precipitation, in place of spray drying or melt extrusion, has the potential to reduce manufacturing timelines and cost[32], as well as allow for the formulation of compounds with poor solubility in volatile organic solvents or high melting-points.[2] Reducing shear conditions during co-precipitation produced a dispersion with increased bulk density, although such a process increased risk of crystallinity. Instead, generating cPAD under high-shear conditions eliminated crystallinity in the dispersion, and heating the cPAD material via an anti-solvent wash produced a material amenable to delivery in suspension formulations as well as with improved mechanical properties and flow to enable direct compression. Such a two-step process allowed for control over temperature and convective mixing during the precipitation step and a separate step to optimize powder properties of the cPAD. This hot wash unit operation could also be coupled with particle coating[25, 35] to generate hierarchical particles for additional improvements to performance. Future work will continue to leverage this procedure to generate densified cPAD for a range of chemical entities and at increasing scale to support clinical studies and commercial manufacturing.

Supplementary Information The online version contains supplementary material available at https://doi.org/10.1007/s11095-022-03416-6.

Acknowledgements The authors acknowledge Steve Crowley, Jim DiNunzio, Edi Meco, and Graciela Terife for work producing the Compound X SDI, Sebastian Escotet, Prapti Kafle, Grace Okoh, Andrew Parker, and Laura Wareham for engaging discussions in the preparation of this work, and Erin Guidry, Joe Kukura, Matthew Lamm, Ian Mangion, Becky Ruck, and Neil Strotman for support.

Funding This work was funded by Merck & Co., Inc., Rahway, NJ, USA.

Declarations

Conflicts of Interest The authors declare no conflicts of interest. The authors are employees of Merck & Co. Inc, Rahway, NJ, USA. Merck & Co. Inc. had no role in the design of the study; in the collection, analyses, or interpretation of data; in the writing of the manuscript; or in the decision to publish the results.

References

1. Baghel S, Cathcart H, O'Reilly NJ. Polymeric amorphous solid dispersions: a review of amorphization, crystallization, stabilization, solid-state characterization, and aqueous solubilization of biopharmaceutical classification system class II drugs. J Pharm Sci. 2016;105(9):2527–44.
2. Shah N, Sandhu H, Choi DS, Chokshi H, Malick AW. Amorphous solid dispersions Theory and Practice. Berlin, Germany: Springer; 2014.
3. Yu L. Amorphous pharmaceutical solids: preparation, characterization and stabilization. Adv Drug Deliv Rev. 2001;48(1):27–42.
4. Jermain SV, Brough C, Williams RO III. Amorphous solid dispersions and nanocrystal technologies for poorly water-soluble drug delivery–an update. Int J Pharm. 2018;535(1–2):379–92.
5. Moseson DE, Taylor LS. The application of temperature-composition phase diagrams for hot melt extrusion processing of amorphous solid dispersions to prevent residual crystallinity. Int J Pharm. 2018;553(1–2):454–66.
6. LaFountaine JS, McGinity JW, Williams RO. Challenges and strategies in thermal processing of amorphous solid dispersions: a review. AAPS PharmSciTech. 2016;17(1):43–55.
7. Ziaee A, Albadarin AB, Padrela L, Faucher A, O'Reilly E, Walker G. Spray drying ternary amorphous solid dispersions of ibuprofen–An investigation into critical formulation and processing parameters. Eur J Pharm Biopharm. 2017;120:43–51.
8. Williams HD, Trevaskis NL, Charman SA, Shanker RM, Charman WN, Pouton CW, *et al*. Strategies to address low drug solubility in discovery and development. Pharmacol Rev. 2013;65(1):315–499.
9. Lee Y-C, McNevin M, Ikeda C, Chouzouri G, Moser J, Harris D, *et al*. Combination of colloidal silicon dioxide with spray-dried solid dispersion to facilitate discharge from an agitated dryer. AAPS PharmSciTech. 2019;20(5):1–7.
10. Poozesh S, Setiawan N, Arce F, Sundararajan P, Della Rocca J, Rumondor A, *et al*. Understanding the process-product-performance interplay of spray dried drug-polymer systems through complete structural and chemical characterization of single spray dried particles. Powder Technol. 2017;320:685–95.
11. Honick M, Das S, Hoag SW, Muller FX, Alayoubi A, Feng X, *et al*. The effects of spray drying, HPMCAS grade, and compression speed on the compaction properties of itraconazole-HPMCAS spray dried dispersions. Eur J Pharm Sci. 2020;155: 105556.

12. Patel S, Kou X, Hou HH, Huang YB, Strong JC, Zhang GG, *et al*. Mechanical properties and tableting behavior of amorphous solid dispersions. J Pharm Sci. 2017;106(1):217–23.
13. Démuth B, Nagy ZK, Balogh A, Vigh T, Marosi G, Verreck G, *et al*. Downstream processing of polymer-based amorphous solid dispersions to generate tablet formulations. Int J Pharm. 2015;486(1–2):268–86.
14. Ekdahl A, Mudie D, Malewski D, Amidon G, Goodwin A. Effect of spray-dried particle morphology on mechanical and flow properties of felodipine in PVP VA amorphous solid dispersions. J Pharm Sci. 2019;108(11):3657–66.
15. Brown C, DiNunzio J, Eglesia M, Forster S, Lamm M, Lowinger M, *et al*. Hot-melt extrusion for solid dispersions: composition and design considerations. Amorphous Solid Dispersions: Springer; 2014. p. 197–230.
16. Breitenbach J. Melt extrusion: from process to drug delivery technology. Eur J Pharm Biopharm. 2002;54(2):107–17.
17. Schenck LR, Lamberto DJ, Kukura IJL, Guzman FJ, Cote A, Koynov A. Process for preparing pharmaceutical compositions. United States patent application US 16/061,513. 2020.
18. Hou HH, Rajesh A, Pandya KM, Lubach JW, Muliadi A, Yost E, *et al*. Impact of method of preparation of amorphous solid dispersions on mechanical properties: Comparison of coprecipitation and spray drying. J Pharm Sci. 2019;108(2):870–9.
19. Sturm DR, Moser JD, Sundararajan P, Danner RP. Spray drying of hypromellose acetate succinate. Ind Eng Chem Res. 2019;58(27):12291–300.
20. Al-Khattawi A, Bayly A, Phillips A, Wilson D. The design and scale-up of spray dried particle delivery systems. Expert Opin Drug Deliv. 2018;15(1):47–63.
21. Poozesh S, Mahdi JS. Are traditional small-scale screening methods reliable to predict pharmaceutical spray drying? Pharm Dev Technol. 2019;24(7):915–25.
22. Dong Z, Chatterji A, Sandhu H, Choi DS, Chokshi H, Shah N. Evaluation of solid state properties of solid dispersions prepared by hot-melt extrusion and solvent co-precipitation. Int J Pharm. 2008;355(1–2):141–9.
23. Simonelli A, Mehta S, Higuchi W. Dissolution rates of high energy sulfathiazole-povidone coprecipitates II: characterization of form of drug controlling its dissolution rate via solubility studies. J Pharm Sci. 1976;65(3):355–61.
24. Sertsou G, Butler J, Hempenstall J, Rades T. Solvent change coprecipitation with hydroxypropyl methylcellulose phthalate to improve dissolution characteristics of a poorly water-soluble drug. J Pharm Pharmacol. 2002;54(8):1041–7.
25. Schenck L, Boyce C, Frank D, Koranne S, Ferguson HM, Strotman N. Hierarchical Particle Approach for Co-Precipitated Amorphous Solid Dispersions for Use in Preclinical In Vivo Studies. Pharmaceutics. 2021;13(7):1034.
26. Jia W, Yawman PD, Pandya KM, Sluga K, Ng T, Kou D, *et al*. Assessing the interrelationship of microstructure, properties, drug release performance, and preparation process for amorphous solid dispersions via noninvasive imaging analytics and material characterization. Pharma Res. 2022:1–18.
27. Song S, Wang C, Wang S, Siegel RA, Sun CC. Efficient development of sorafenib tablets with improved oral bioavailability enabled by coprecipitated amorphous solid dispersion. Int J Pharma. 2021;610:121216.
28. Shah N, Iyer RM, Mair H-J, Choi D, Tian H, Diodone R, *et al*. Improved human bioavailability of vemurafenib, a practically insoluble drug, using an amorphous polymer-stabilized solid dispersion prepared by a solvent-controlled coprecipitation process. J Pharm Sci. 2013;102(3):967–81.
29. Frank D, Schenck L, Koynov A, Su Y, Li Y, Variankaval N. Optimizing Solvent Selection and Processing Conditions to Generate High Bulk-Density, Co-Precipitated Amorphous Dispersions of Posaconazole. Pharmaceutics. 2021;13(12):2017.
30. Frank D, Nie H, Chandra A, Coelho A, Dalton C, Dvorak H, *et al*. High bulk-density amorphous dispersions to enable direct compression of reduced image size amorphous dosage units. J Pharma Sci. 2022. in press.
31. Schenck L, Koynov A, Cote A. Particle engineering at the drug substance, drug product interface: a comprehensive platform approach to enabling continuous drug substance to drug product processing with differentiated material properties. Drug Dev Ind Pharm. 2019;45(4):521–31.
32. Strotman NA, Schenck L. Coprecipitated amorphous dispersions as drug substance: opportunities and challenges. Org Process Res Dev. 2022;26(1):10–3.
33. Matteucci ME, Hotze MA, Johnston KP, Williams RO. Drug nanoparticles by antisolvent precipitation: mixing energy versus surfactant stabilization. Langmuir. 2006;22(21):8951–9.
34. Harter A, Schenck L, Lee I, Cote A. High-shear rotor–stator wet milling for drug substances: expanding capability with improved scalability. Org Process Res Dev. 2013;17(10):1335–44.
35. Schenck L, Mann AKP, Liu Z, Milewski M, Zhang S, Ren J, *et al*. Building a better particle: Leveraging physicochemical understanding of amorphous solid dispersions and a hierarchical particle approach for improved delivery at high drug loadings. Int J Pharm. 2019;559:147–55.
36. Gamble JF, Chiu W-S, Tobyn M. Investigation into the impact of sub-populations of agglomerates on the particle size distribution and flow properties of conventional microcrystalline cellulose grades. Pharm Dev Technol. 2011;16(5):542–8.
37. Horio T, Yasuda M, Matsusaka S. Effect of particle shape on powder flowability of microcrystalline cellulose as determined using the vibration shear tube method. Int J Pharm. 2014;473(1–2):572–8.
38. Barjat H, Checkley S, Chitu T, Dawson N, Farshchi A, Ferreira A, *et al*. Demonstration of the feasibility of predicting the flow of pharmaceutically relevant powders from particle and bulk physical properties. J Pharm Innov. 2021;16(1):181–96.
39. Bhujbal SV, Pathak V, Zemlyanov DY, Taylor LS, Zhou QT. Physical stability and dissolution of lumefantrine amorphous solid dispersions produced by spray anti-solvent precipitation. J Pharm Sci. 2021;110(6):2423–31.
40. Ikeda C, Zhou G, Lee Y-C, Chouzouri G, Howell L, Marshall B, *et al*. Application of online NIR spectroscopy to enhance process understanding and enable in-process control testing of secondary drying process for a spray-dried solid dispersion intermediate. J Pharma Sci. 2022;111(9):2540–51.
41. Lowinger M, Baumann J, Vodak DT, Moser J. Practical considerations for spray dried formulation and process development. Discovering and developing molecules with optimal drug-like properties: Springer; 2015. p. 383–435.
42. Cote A, Sirota E. CRYSTALLIZATION: the pursuit of a robust approach for growing crystals directly to target size. American Pharmaceutical Review. 2010;13(7):46.
43. Meng W, Sirota E, Feng H, McMullen JP, Codan L, Cote AS. Effective Control of Crystal Size via an Integrated Crystallization, Wet Milling, and Annealing Recirculation System. Org Process Res Dev. 2020;24(11):2639–50.
44. Hancock BC, Zografi G. Characteristics and significance of the amorphous state in pharmaceutical systems. J Pharm Sci. 1997;86(1):1–12.
45. Debenedetti PG, Stillinger FH. Supercooled liquids and the glass transition. Nature. 2001;410(6825):259–67.
46. Krishna Kumar N, Suryanarayanan R. Crystallization propensity of amorphous pharmaceuticals: kinetics and thermodynamics. Mol Pharma. 2022;19(2):472–83.

47. Indulkar AS, Lou X, Zhang GG, Taylor LS. Insights into the dissolution mechanism of ritonavir–copovidone amorphous solid dispersions: importance of congruent release for enhanced performance. Mol Pharm. 2019;16(3):1327–39.
48. Newman A, Zografi G. What are the important factors that influence API crystallization in miscible amorphous API–excipient mixtures during long-term storage in the glassy state? Mol Pharma. 2021;19(2):378–91.
49. Friesen DT, Shanker R, Crew M, Smithey DT, Curatolo W, Nightingale J. Hydroxypropyl methylcellulose acetate succinate-based spray-dried dispersions: an overview. Mol Pharm. 2008;5(6):1003–19.
50. Wuelfing WP, El Marrouni A, Lipert MP, Daublain P, Kesisoglou F, Converso A, *et al*. Dose number as a tool to guide lead optimization for orally bioavailable compounds in drug discovery. J Med Chem. 2022;65(3):1685–94.

Publisher's Note Springer Nature remains neutral with regard to jurisdictional claims in published maps and institutional affiliations.

Springer Nature or its licensor (e.g. a society or other partner) holds exclusive rights to this article under a publishing agreement with the author(s) or other rightsholder(s); author self-archiving of the accepted manuscript version of this article is solely governed by the terms of such publishing agreement and applicable law.